The Journal of Experimental Biology 211, 1958-1963
Published by The Company of Biologists 2008
doi:10.1242/jeb.014308

# Terminal contact elements of insect attachment devices studied by transmission X-ray microscopy

T. Eimüller[1,2], P. Guttmann[3] and S. N. Gorb[2,*]

[1]Junior Research Group Magnetic Microscopy, Experimental Physics, University of Bochum, D-44780 Bochum, Germany, [2]Evolutionary Biomaterials Group, Department for Thin Films and Biological Systems, Max Planck Institute for Metals Research, Heisenbergstr. 3, D-70569 Stuttgart, Germany and [3]University of Göttingen c/o BESSY GmbH, Albert-Einstein-Str. 15, 12489 Berlin, Germany

*Author for correspondence (e-mail: s.gorb@mf.mpg.de)

Accepted 20 March 2008

## SUMMARY

**For the first time, the terminal elements (spatulae) of setal (hairy) attachment devices of the beetle *Gastrophysa viridula* (Coleoptera, Chrysomelidae) and the fly *Lucilia caesar* (Diptera, Calliphoridae) were studied using transmission X-ray microscopy (TXM) with a lateral resolution of about 30 nm. Since images are taken under ambient conditions, we demonstrate here that this method can be applied to study the contact behaviour of biological systems, including animal tenent setae, in a fresh state. We observed that the attached spatulae show a viscoelastic behavior increasing the contact area and providing improved adaptability to the local topography of the surface. The technique can be extended to TXM tomography, which would provide three-dimensional information and a deeper insight into the details of insect attachment structures.**

Key words: attachment, adhesion, beetle, *Gastrophysa viridula*, Coleoptera, Chrysomelidae, fly, *Lucilia caesar*, Diptera, Calliphoridae, contact formation, transmission X-ray microscope, TXM.

## INTRODUCTION

Different hypotheses ranging from adhesive fluids, microsuckers or electrostatic forces have been proposed to explain the mechanism by which some animals adhere to and walk on vertical walls and even on ceilings (Gillett and Wigglesworth, 1932; Maderson, 1964). However, careful experiments, demonstrating functional principles behind biological attachment devices, have been performed only in recent years (Stork, 1980; Walker et al., 1985; Autumn et al., 2000; Gorb and Scherge, 2000; Langer et al., 2004; Huber et al., 2005). Such studies revealed that attachment of geckoes is based on van der Waals forces (Hiller, 1968; Autumn et al., 2000) and possibly wetting phenomena which might mediate adhesion (Huber et al., 2005). Insects, however, mostly rely on capillary forces with some contribution of van der Waals interactions (Walker et al., 1985; Federle et al., 2001; Langer et al., 2004). Two types of animal pads have been identified as being required for these attachments: (1) those consisting of a soft, deformable material with a smooth surface structure, so-called arolia and euplantulae, which occur in cockroaches, grasshoppers, bees, ants and bugs (Roth and Willis, 1952; Slifer, 1950; Ghasi-Bayat and Hasenfuss, 1980; Gorb, 2001; Jiao et al., 2000; Federle et al., 2001; Gorb and Gorb, 2004), and (2) those with a contact area subdivided into thousands of cuticular hairs, so called setae, with a diameter in the micrometer range (Stork, 1983; Gorb, 1998; Beutel and Gorb, 2001). In the case of the hairy attachment devices, contact between the attachment pad and substrate is established in a large number of small contact areas (Scherge and Gorb, 2001). The setal strategy is a more recent evolutionary development in insects than the smooth surface one, and is present in flies, beetles, dobsonflies and earwigs. The small, flexible setae can easily adapt to the local texture of a rough natural surface, and thus increase the number of contacting microsites between the pad and substrate. In addition, setae bear disk-like or spatula-like terminal structures responsible for contact formation (Stork, 1983). Our previous study revealed that the density of such potential contact sites increases with the body mass (Scherge and Gorb, 2001). A house fly has about 6000 contacting sites, each about 2 μm in size, whereas a gecko foot has about 500 000 contact hairs, all subdivided in hundreds of spatula-shaped terminations with a lateral dimension of about 0.2–0.5 μm.

Previous theoretical approximations have predicted that spatulae must be an essential feature for intimate contact formation between the attachment pads and substrate and thus for generation of strong adhesive forces (Persson and Gorb, 2003). Also, recent experimental studies have shown that the surface area of the spatula increases when in contact with the substrate compared with the non-contact state (Niederegger et al., 2002). Owing to the ability to spread spatulae in contact, geckoes rely more on the peeling mode of contact (Kendall, 1975; Tian et al., 2006) than on the Johnson-Kendall-Roberts mode (Johnson et al., 1971; Autumn et al., 2000; Arzt et al., 2003). To provide new insights in the role of the spatula in proper contact formation new techniques are required to visualize spatulae in contact. Direct visualization of the underlying contact mechanisms can be obtained with only a very few imaging techniques, each having some restrictions. The number, orientation and the external structure of the setae has been observed by optical microscopy (Stork, 1983), by scanning electron microscopy (SEM) (Walker et al., 1985; Gorb, 1998), by transmission electron microscopy (TEM) (Gorb, 1998) and by atomic force microscopy (AFM) (Langer et al., 2004). However, all these methods become problematic for studies of spatulae in a newly established contact with a surface under ambient conditions. In optical microscopy, the lateral resolution is limited by diffraction to about 300 nm. Since the width of the setae is close to this limit, details of the contact area cannot be studied. Transmission electron microscopes have much better

spatial resolution; however, the object has to be exposed to a high vacuum. As a consequence, the setae must be dried and cannot be imaged under natural conditions. Environmental scanning electron microscopy (ESEM) and atomic force microscopy (AFM) allow studies under ambient conditions, but not in transmission. The latter is also true for cryo-SEM, which seems to be a very good method to observe contacting setae from above (Gorb, 2006), but potential artefacts of the cryofixation processes on the adhesive setae are not well known yet. To overcome all these problems in the present study we used transmission soft X-ray microscopy (Niemann et al., 1976; Kirz et al., 1995; Schmahl et al., 1996) which provides a means of studying setae in fresh contact and under ambient conditions, i.e. in air and at room temperature with a lateral resolution better than 30 nm.

## MATERIALS AND METHODS

The experiments described here were performed with a full-field transmission X-ray microscope using the undulator beamline U41 of the synchrotron source BESSY II in Berlin (Guttmann et al., 2003). The object is illuminated by a condenser with dynamical aperture synthesis, i.e. a pair of rotating mirrors, which destroys the lateral cohesion of the undulator radiation and matches the aperture to the image-forming micro zone plate. Soft X-rays with an energy of 524.5 eV were used, located in the so called 'water window' between the K absorption edges of the elements carbon (277 eV) and oxygen (543.1 eV). Close to the K absorption edge of oxygen a large natural contrast between carbon-containing substances and air or water can be obtained without staining (Wolter, 1952). X-rays with this energy have, in water, a mean free path of about 10 μm, allowing biological systems to be studied in their natural environment, e.g. cells in water (Kirz et al., 1995; Schmahl et al., 1996). The transmitted X-rays are detected by a direct back-illuminated charge-coupled device (CCD) camera without an antireflective coating. Its chip is a two dimensional array of 1024×1024 pixels, each of which acts as an integrating X-ray detector. The signal obtained from each pixel is directly proportional to the number of detected X-ray photons. The quantum detection efficiency (DQE) was previously determined (Wilhein et al., 1994). Therefore, this camera is a calibrated system useable for quantitative measurements. The large electron capacity of each pixel ($4\times10^5$ $e^-$) together with the low readout noise (10 $e^-$ for integration times below 30 s) and the small dark current [2.9 $e^-$/(pixels $s^{-1}$)] leads to a high dynamic range of $4.4\times10^3$ at E=520 eV (Wilhein et al., 1994), which makes it possible to study strongly absorbing features close to low absorbing ones.

In our experiments, the setae were attached to a 100 nm thick commercial $Si_3N_4$ membrane (Silson Ltd, Blisworth, UK). Such a thin substrate is necessary to obtain sufficiently high transmission (~80%) of the soft X-rays. The transmitted light is imaged by a Fresnel micro zone plate (MZP). This X-ray lens is a circular grating with a radially increasing line density. The width of the outermost zone determines the resolution. The MZP used in this study has an outermost zone width of 25 nm which enables resolution of structures smaller than 30 nm. Since transmission X-ray microscopy (TXM) works in the transmission mode, information is integrated over the whole thickness of the object.

Distal tarsomeres of the beetle *Gastrophysa viridula* De Geer (Coleoptera, Chrysomelidae) and the fly *Lucilia caesar* Linnaeus (Diptera, Calliphoridae) were separated from the body and attached to the $Si_3N_4$ membrane by imitating the natural motion of the attaching leg (Niedreegger and Gorb, 2003), under a light microscope. After preparation, the sample was mounted immediately into the TXM so that setae in contact with the membrane could be imaged within 10 min. Beetles and flies bear several different types of setae with variously shaped terminal parts (plus some transitory shapes) (Stork, 1983; Gorb, 1998), however, in this study, we mostly concentrated on the spatula-like terminal parts.

Using TXM imaging it is possible to quantitatively measure the thickness of an object. If X-rays with an intensity $I_0$ pass through a material with absorption coefficient μ and thickness $z$, then the transmitted intensity $I$ is described by Beer's law: $I=I_0\exp(-\mu z)$. Because of the linear behaviour of the detector used every pixel value recorded by the CCD camera is directly proportional to the intensity $I$ of X-rays transmitted through the object. To determine the thickness $z$ of a seta we record the intensity distribution $I(n)$ along a line of pixels $n$. As the X-ray magnification and the physical size of a pixel are known, the distance $x$ along the recorded line can be expressed in nanometres. The obtained distribution, $I(x)$, is called a 'line scan'. To detect the intensity distribution of the illuminating radiation in front of the absorber, $I_0(x)$, we take an image without a sample, a so called 'flat field', before we start mounting the sample. The normalization $I(x)/I_0(x)$ corrects not only for the nonhomogeneous illumination profile but also for small variations in the sensitivity of different pixels of the CCD camera. An additional correction is necessary since the beam profile in the synchrotron changes slightly over some minutes: $I_0(x,t)=I_0(x)+\Delta I_0(x,t)$. To determine $\Delta I_0(x,t)$ at the time $t$ of the measurement, we assume that this small correction term can be approximated by a linear function of $x$, which we fit to the intensity distribution of the line scan for x values outside the object, $x_{out}$. In other words, the intensity next to the object, $I(x_{out},t)=I_0(x_{out},t)$, is linearly extrapolated into the object to get $I_0(x,t)$. This procedure also corrects for the absorption due to the sample support foil. Finally, the thickness of the seta along a line, $z(x)$, is calculated by conversion of Beer's law: $z(x)=-\mu^{-1}\ln[I(x)/I_0(x,t)]$. The absorption coefficient of the seta is assumed to be that of chitin, which has been calculated, for the energy used of 524.5 eV, as $\mu=1.00\ \mu m^{-1}$, assuming a homogeneous density of 1.35 g $cm^{-3}$ and a chemical composition of $C_8H_{13}O_5N$.

For transmission electron microscopy, tarsomeres of the beetle *Gastrophysa viridula* were fixed for 12 h at 4°C in 2.5% glutaraldehyde (in 0.01 mol $l^{-1}$ phosphate buffer at pH 7.3), and postfixed for 1 h in 1% osmium tetroxide in phosphate buffer at 2°C. After washing, preparations were stained for 1 h at 4°C in 0.1% aqueous uranyl acetate solution, washed, dehydrated, and embedded in a low viscosity resin (Spurr, 1969). Ultrathin sections were picked up on copper grids coated with formvar film. Sections were stained with uranyl acetate and lead citrate, and observations were made with a Philips CM10 transmission electron microscope at 60 kV.

## RESULTS

An example of the SEM image of the dry beetle spatula in contact with a surface is shown in Fig. 1. It can be clearly seen that the spatula establishes a plate-like contact, which can be separated only by using the peeling separation mode. A pattern of longitudinal ribs and grooves is present on the back (dorsal) side of the terminal plate.

TXM imaging revealed that not all setae are attached to the membrane. This can partly be ascribed to the imperfect imitation of the movement of an insect's leg during attachment. Whether setae are in contact with the substrate or not can clearly be distinguished by the fact that those not attached to the surface vibrate and thus are blurred in images exposed for longer than 2 s, whereas attached hairs do not move and have sharper contours. Free, non-contacting setae and attached setae of the beetle *G. viridula* have different

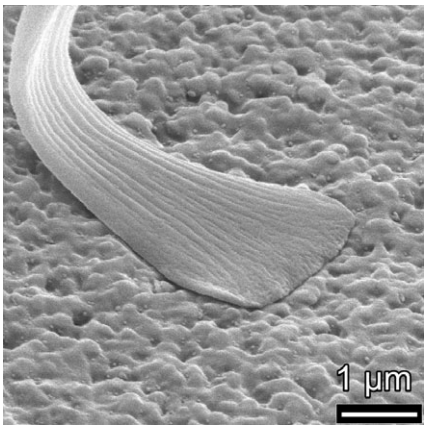


Fig. 1. Scanning electron microscopy (SEM) image of the spatula-like terminal contact element of the beetle *Gastrophysa viridula* while in contact with a rough substrate. The thin, band-like fine structure of the spatula spreads over the surface. This preparation was dried prior to SEM imaging.

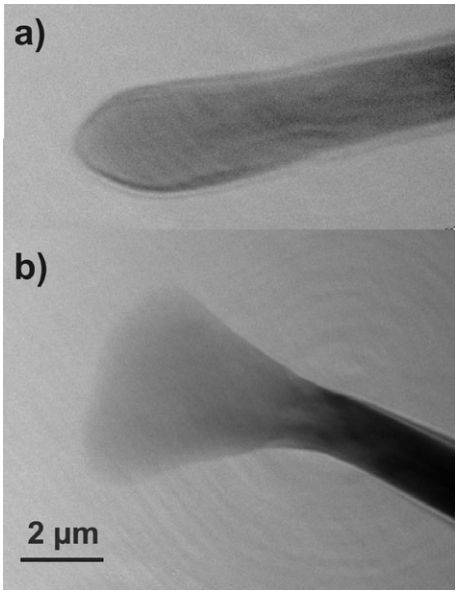


Fig. 2. Transmission X-ray microscopy (TXM) images of setae in the beetle *Gastrophysa viridula* (a) not in contact and (b) in a fresh contact with a $Si_3N_4$ membrane surface. Please note changes in the shape and optical density of spatula. The optical density scales with the thickness of the material, if one assumes the same density of the material of the spatula.

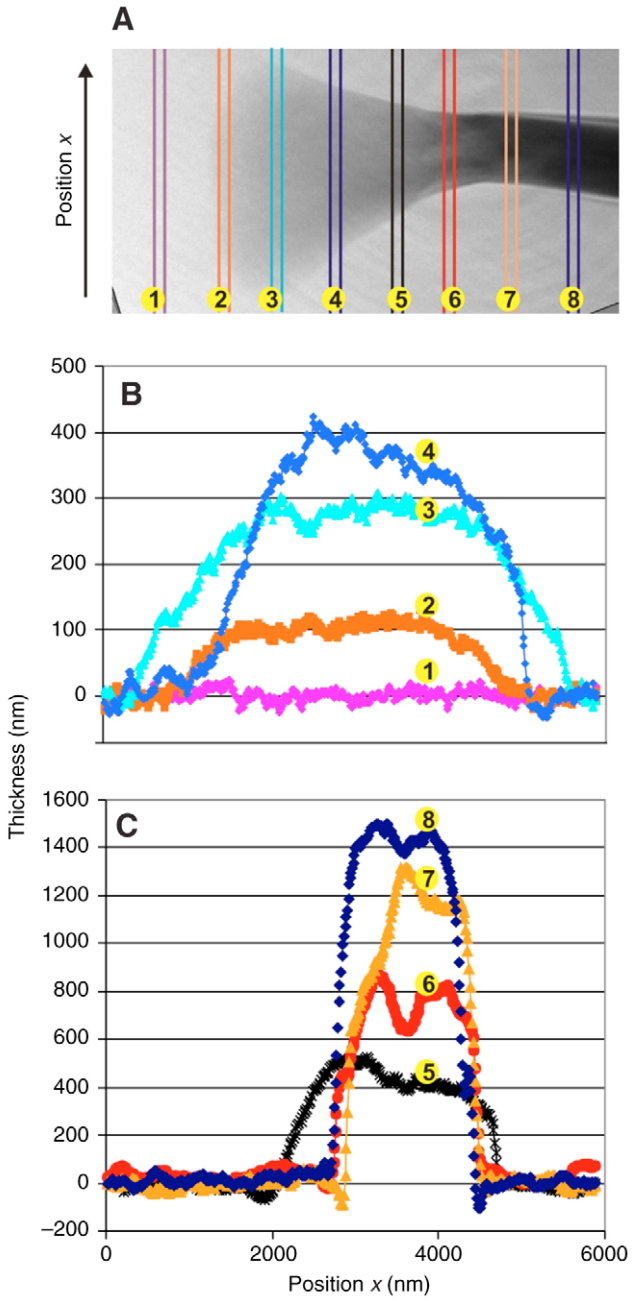


Fig. 3. Measurement of the thickness of a seta from the beetle *Gastrophysa viridula* in contact with the substrate. (A) TXM image of the spatula region of a seta, in contact with a $Si_3N_4$ membrane surface. (B,C) Line scans taken at the positions 1–8, as marked in A. To increase the signal to noise ratio, the scans have been averaged between the two lines of each position.

shapes (Fig. 2). A seta that is not in contact with the membrane is narrower at the tip (Fig. 2a) than the one that is attached to the $Si_3N_4$ membrane (Fig. 2b). The effective contact area was estimated to be 4.7 µm$^2$. The lower contrast indicates a low thickness of the spatula especially in its distal part. Quantitative information on the thickness distribution is revealed by a series of line scans of a seta in contact with the surface. They show that the thickness in the contact area continuously decreases until it reaches a terminal value of only about 100 nm (Fig. 3). The consistency of the thickness calibration by Beer's law can be seen in line scan 8 of Fig. 3C, taken in a non-contact area of the seta. At this position, where the cross-section is expected to be approximately circular, the structure has a width of 1.5 µm as well as a central thickness of 1.5 µm. The same line scan analysis has been performed for a seta not in contact with the surface. Fig. 4 shows that in this case the thickness is nearly constant along the seta, i.e. it varies only between 450 and 600 nm. Towards the distal end only a slight reduction in the thickness can be observed. Line scan 2, recorded 600 nm from the tip of the seta, has a thickness of about 400 nm. Note also that the width of the non-contact seta is nearly constant with a value of about 2.7 µm. By contrast, the seta in contact with the surface may increase its width from 1.5 µm to 4.7 µm towards the tip (Fig. 3). Transmission electron microscopy has demonstrated that the beetle spatula is not a solid structure, but

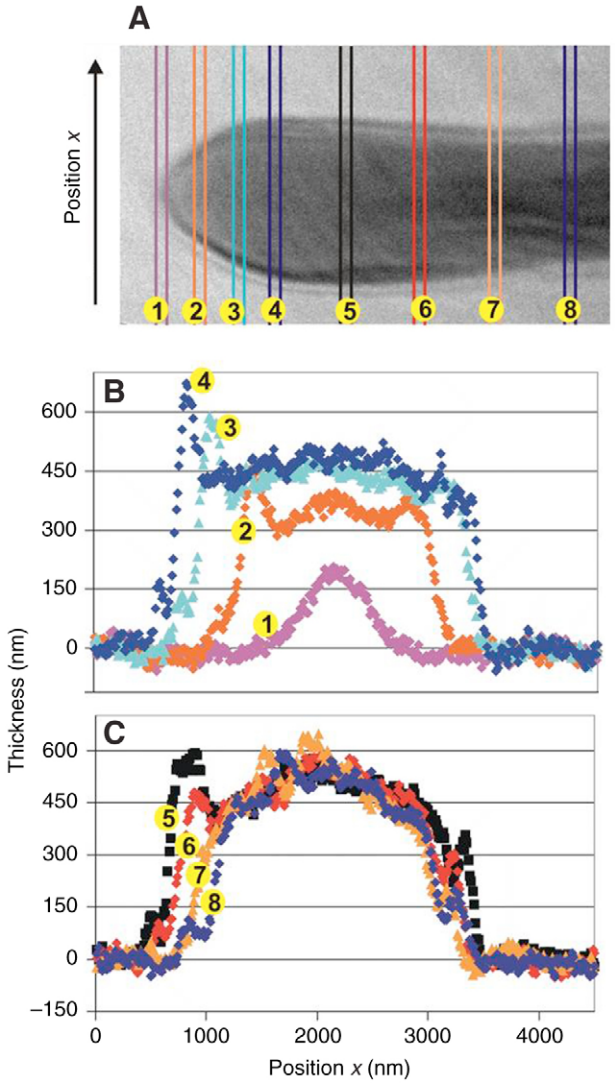


Fig. 4. Measurement of the thickness of a seta from the beetle *Gastrophysa viridula* not in contact with the substrate. (A) TXM image of the spatula region of a seta which is not in contact with the surface. (B,C) Line scans taken at positions 1–8, as marked in A. To increase the signal to noise ratio, the scans have been averaged between the two lines of each position.

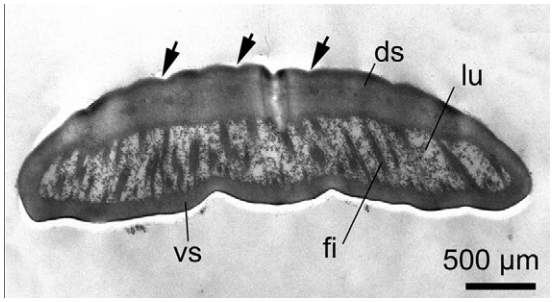


Fig. 5. Transmission electron micrograph of the cross-section of a spatula from the beetle *Gastrophysa viridula*. Arrows indicate corrugations on the dorsal surface. ds, dorsal surface; fi, nanofibres; lu, lumen filled with the secretion; vs, ventral surface.

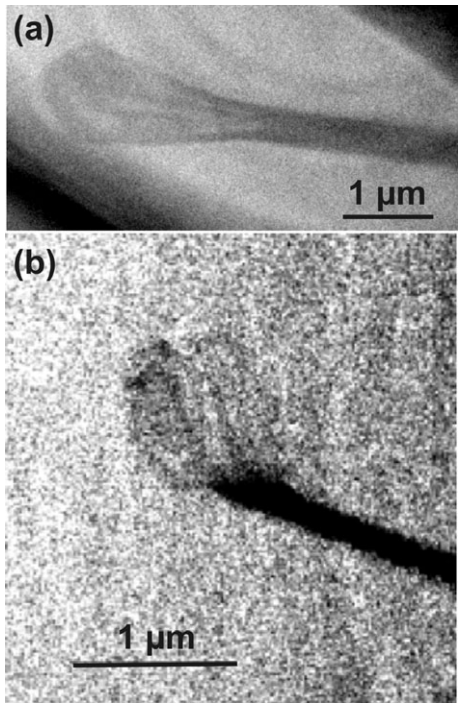


Fig. 6. (a) TXM image of a seta of the fly *Lucilia caesar* in contact with a $Si_3N_4$ membrane. (b) Another seta at higher magnification. In both cases a groove-like ultrastructure, running longitudinally, can be observed in the contact region.

contains a lumen filled with secretory fluid. The thicker dorsal wall (300–400 nm) is connected with the thinner ventral one (100–120 nm) by an array of nanofibres with a thickness of 40–70 nm. The dorsal wall contains light corrugations as can be seen in transmission electron micrographs (Fig. 5).

Similar behaviour of spatulae in contact was observed in the fly *L. caesar* (Fig. 6). An increase of the area of the spatula, while in contact, by comparison with non-contacting spatulae, was also seen. In addition, TXM images revealed a groove-like ultrastructure, running longitudinally along the spatula, in the contact region.

## DISCUSSION

This paper has demonstrated that TXM provides a means of studying the contact behaviour of hairy attachment systems of insects with a high lateral resolution. We have obtained images with a lateral resolution of about 30 nm, however, with the best currently available zone plates even 15 nm should be possible (Chao et al., 2005). Since images were taken under ambient conditions, a native biological material of insect setae could be studied, and thus being very close to their natural behaviour. In the transmission mode of visualization, this is hardly possible with any other existing technique. In addition, the thickness of the material can be determined with a resolution of about 20 nm, only limited by photon noise and by uncertainties of the absorption coefficient $\mu$, which can be overcome in the future by experimental determination.

We have previously applied a freezing-substitution technique in order to estimate contact area of single spatulae of the fly *Calliphora vicina* (Diptera, Calliphoridae) (Niederegger et al., 2002). This method is presumably not free of artefacts caused by a combination of freezing, chemical fixation and drying, but until recently, there was no other way to provide these results. The presented TXM

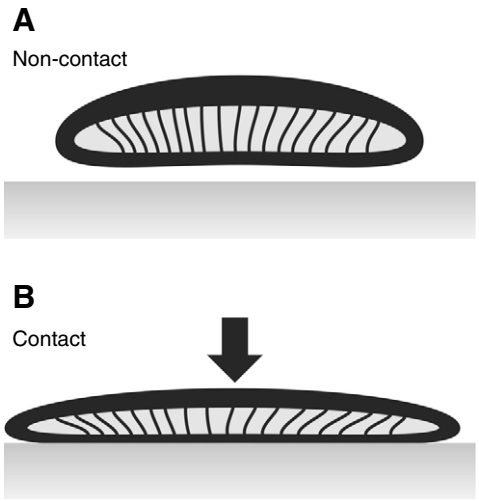


Fig. 7. Diagram showing hypothetical deformation of the spatula, in the cross-section, during contact with a substrate. (A) The spatula in a non-contact state. (B) The spatula in a contact state. The diagram is based on findings from TXM and TEM.

method supports previously obtained data on the area change of the spatula on contact by 25–30% (Niederegger et al., 2002). The determined thickness of the distal end of the spatula in contact corresponds to estimations obtained from SEM (Fig. 1) and TEM studies (Gorb, 1998) (present study).

The finding that contacting and non contacting setae have different shape and thickness would suggest that spatulae behave viscoelastically, i.e. the material at the end of each spatula 'flows' during attachment. This leads to an increase in the contact area between the spatula and substrate and to an enhanced adaptability to the local topography of the surface (Niederegger et al., 2002). Such an adaptability of the thin plate of the spatula to the substrate unevenness in micro- and nanometre ranges was previously theoretically supported as one of the key mechanisms responsible for strong adhesion in biological hairy attachment devices (Persson and Gorb, 2003). Spatulae in contact demonstrate a gradient of thickness, i.e. extremely thin at the tip of the spatula and at least four times thicker at the base (Fig. 3). This gradient can be explained as an optimization between plate adaptability and resistance against mechanical damages.

Transmission electron microscopy of cross-sections of beetle spatulae has revealed unusual ultrastructure, previously unknown from other hairy attachment devices including those of geckos (Persson and Gorb, 2003) and flies (Bauchhenss, 1979; Gorb, 1998). In the spatula the combination of the thin walls filled out with a fluid and internal nanofibres makes it possible to explain deformations caused by contact formation as observed in the TXM (Fig. 7). Since the dorsal wall of the spatula is thicker than the ventral one, it deforms less under compression or shear and acts as a kind of a stable mechanical support for the thin flexible ventral wall, suspended from the dorsal wall through nanofibres. This architecture resembles a sandwich-like ultrastructure previously described for smooth adhesive pads having a number of specific functional features (for a review, see Gorb, 2008). The internal structure of the spatula, consisting of fibres and fluid, may be responsible for the viscoelastic properties of the spatula as previously shown for adhesive pads of grasshoppers (Gorb et al., 2000).

Setae of the fly *L. caesar* have a groove-like ultrastructure on the dorsal side of the spatula. Similar structures have been shown previously by SEM in other fly species (Gorb, 1998) and earwigs (Haas and Gorb, 2004). Grooves may stabilize the thin film-like structure in contact with the surface and/or may help in the process of attachment by spreading over the surface. Additionally, the roughness of the pattern of grooves and ribs may decrease condensation of spatulae (Peressadko and Gorb, 2004; Huber et al., 2007). The TEM study shows that dorsal corrugations in beetles are presumably not drying artefacts. These structures are hardly seen in TXM, and were clearly visualised by this method only in flies.

It would be desirable to extend the technique presented here to TXM tomography (Weiss et al., 2000; Larabell and Le Gros, 2004; Attwood, 2006) which will produce three dimensional images that will provide a deeper insight into the details of insect attachment structures. However, for high resolution tomography a hundred and more images from different angles need to be recorded, which would take hours. Thus, for fresh contact studies only low resolution tomography may be possible. X-ray stability of the unfixed setae is another challenge. In our study we observed X-ray-induced damage after taking more than about ten images of the same object. This problem may be reduced by cryo-TXM (Schneider, 1998) or scanning transmission X-ray microscopy (STXM) (Rarback et al., 1984; Kirz et al., 1995). Since in STXM there is no low-efficiency micro zone plate between the object and the detector, images can be recorded at a lower X-ray dose.

This study was supported by a grant from the Federal Ministry of Education, Science and Technology, Germany to S.G. (project InspiRat 01RI0633D).

## REFERENCES

**Arzt, E., Gorb, S. and Spolenak, R.** (2003). From micro to nano contacts in biological attachment devices. *Proc. Natl. Acad. Sci. USA* **100**, 10603-10606.
**Attwood, D.** (2006). Nanotomography comes of age. *Nature* **442**, 642-643.
**Autumn, K., Liang, Y. A., Hsieh, S. T., Zesch, W., Chan, W. P., Kenny, T. W., Fearing, R. and Full, R. J.** (2000). Adhesive force of a single gecko foot-hair. *Nature* **405**, 681-685.
**Bauchhenss, E.** (1979). Die Pulvillen von *Calliphora erythrocephala* Meig. (Diptera, Brachycera) als Adhäsionsorgane. *Zoomorphologie* **93**, 99-123.
**Beutel, R. G. and Gorb, S. N.** (2001). Ultrastructure of attachment specializations of hexapods (Arthropoda): evolutionary patterns inferred from a revised ordinal phylogeny. *J. Zoolog. Syst. Evol. Res.* **39**, 177-207.
**Chao, W., Harteneck, B. D., Liddle, J. A., Anderson, E. H. and Attwood, D. T.** (2005). Soft X-ray microscopy at a spatial resolution better than 15 nm. *Nature* **435**, 1210-1213.
**Federle, W., Brainerd, E. L., McMahon, T. A. and Hölldobler, B.** (2001). Biomechanics of the movable pretarsal adhesive organ in ant and bees. *Proc. Natl. Acad. Sci. USA* **98**, 6215-6220.
**Ghasi-Bayat, A. and Hasenfuss, I.** (1980). Zur Herkunft der Adhäsionsflüssigkeit der Tarsalen Haftlappen bei den Pentatomidae (Heteroptera). *Zool. Anz.* **204**, 13-18.
**Gillett, J. D. and Wigglesworth, V. B.** (1932). The climbing organ of an insect, *Rhodnius prolixus* (Hemiptera, Reduviidae). *Proc. R. Soc. Lond. B Biol. Sci.* **111**, 364-376.
**Gorb, S. N.** (1998). The design of the fly adhesive pad: distal tenent setae are adapted to the delivery of an adhesive secretion. *Proc. R. Soc. Lond. B Biol. Sci.* **265**, 747-752.
**Gorb, S. N.** (2001). *Attachment Devices of Insect Cuticle*. Dordrecht: Kluwer Academic Publishers.
**Gorb, S. N.** (2006). Fly microdroplets viewed big: a Cryo-SEM approach. *Microsc. Today* **14**, 38-39.
**Gorb, S. N.** (2008). Smooth attachment devices in insects: functional morphology and biomechanics. In *Insect Mechanics and Control, Volume 34, Advances in Insect Physiology* (ed. J. Casas and S. Simpson), pp. 81-116. London, New York: Elsevier.
**Gorb, S. N. and Gorb, E. V.** (2004). Ontogenesis of the attachment ability in the bug *Coreus marginatus* (Heteroptera, Insecta). *J. Exp. Biol.* **207**, 2917-2924.
**Gorb, S. and Scherge, M.** (2000). Biological microtribology: anisotropy in frictional forces of orthopteran attachment pads reflects the ultrastructure of a highly deformable material. *Proc. R. Soc. Lond. B. Biol. Sci.* **267**, 1239-1244.
**Gorb, S., Jiao, Y. and Scherge, M.** (2000). Ultrastructural architecture and mechanical properties of attachment pads in *Tettigonia viridissima* (Orthoptera Tettigoniidae). *J. Comp. Physiol. A* **186**, 821-831.
**Guttmann, P., Niemann, B., Rehbein, S., Knöchel, C., Rudolph, D. and Schmahl, G.** (2003). The transmission X-ray microscope at BESSY II. *J. Phys. IV France* **104**, 85-90.
**Haas, F. and Gorb, S.** (2004). Evolution of locomotory attachment pads in the Dermaptera (Insecta). *Arthropod Struct. Dev.* **33**, 45-66.

**Hiller, U.** (1968). Untersuchungen zum Feinbau und zur Funktion der Haftborsten von Reptilien. *Z. Morphol. Tiere* **62**, 307-362.
**Huber, G., Mantz, H., Spolenak, R., Mecke, K., Jacobs, K., Gorb, S. N. and Arzt, E.** (2005). Evidence for capillarity contributions to gecko adhesion from single spatula nanomechanical measurements. *Proc. Natl. Acad. Sci. USA* **102**, 16293-16296.
**Huber, G., Gorb, S. N., Hosoda, N., Spolenak, R. and Arzt, E.** (2007). Influence of surface roughness on gecko adhesion. *Acta Biomater.* **3**, 607-610.
**Jiao, Y., Gorb, S. and Scherge, M.** (2000). Adhesion measured on the attachment pads of *Tettigonia viridissima* (Orthoptera, Insecta). *J. Exp. Biol.* **203**, 1887-1895.
**Johnson, K. L., Kendall, K. and Roberts, A. D.** (1971). Surface energy and the contact of elastic solids. *Proc. R. Soc. Lond. A Math. Phys. Sci.* **324**, 301-313.
**Kendall, K.** (1975). Thin-film peeling – the elastic term. *J. Phys. D Appl. Phys.* **8**, 1449-1452.
**Kirz, J., Jacobsen, C. and Howells, M.** (1995). Soft X-ray microscopes and their biological applications. *Q. Rev. Biophys.* **28**, 33-130.
**Langer, M. G., Ruppersberg, J. P. and Gorb, S. N.** (2004). Adhesion forces measured at the level of a terminal plate of the fly's seta. *Proc. R. Soc. Lond. B Biol. Sci.* **271**, 2209-2215.
**Larabell, C. and Le Gros, M. A.** (2004). X-ray tomography generates 3-D reconstructions of the yeast, *Saccharomyces cerevisiae*, at 60 nm resolution. *Mol. Biol. Cell* **15**, 957-962.
**Maderson, P. F. A.** (1964). Keratinized epidermal derivatives as an aid to climbing in gekkonid lizards. *Nature* **203**, 780-781.
**Niederegger, S. and Gorb, S.** (2003). Tarsal movements in flies during leg attachment and detachment on a smooth substrate. *J. Insect Physiol.* **49**, 611-620.
**Niederegger, S., Gorb, S. and Jiao, Y.** (2002). Contact behaviour of tenent setae in attachment pads of the blowfly *Calliphora vicina* (Diptera, Calliphoridae). *J. Comp. Physiol. A* **187**, 961-970.
**Niemann, B., Rudolph, D. and Schmahl, G.** (1976). X-ray microscopy with synchrotron radiation. *Appl. Opt.* **15**, 1883-1884.
**Peressadko, A. and Gorb, S. N.** (2004). Surface profile and friction force generated by insects. In *Fortschritt-Berichte VDI 249* (ed. I. Boblan and R. Bannasch), pp. 257-261. Düsseldorf: VDI Verlag.
**Persson, B. N. J. and Gorb, S. N.** (2003). The effect of surface roughness on the adhesion of elastic plates with application to biological systems. *J. Chem. Phys.* **119**, 11437-11444.
**Rarback, H., Kenney, J. M., Kirz, J., Howells, M. R., Chang, P., Coane, P. J., Feder, R., Houzego, P. J., Kern, D. P. and Sayre, D.** (1984). Recent results from the Stony Brook scanning microscope. In *X-ray Microscopy* (*Vol. 43, Springer Series in Optical Sciences*) (ed. G. Schmahl and D. Rudolph), pp. 203-216. Berlin: Springer-Verlag.
**Roth, L. M. and Willis, E. R.** (1952). Tarsal structure and climbing ability of cockroaches. *J. Exp. Zool.* **119**, 483-517.
**Scherge, M. and Gorb, S. N.** (2001). *Biological Micro- and Nanotribology*. Berlin: Springer.
**Schmahl, G., Rudolph, D., Niemann, B., Guttmann, P., Thieme, J. and Schneider, G.** (1996). *X-ray microscopy. Naturwissenschaften* **83**, 61-70.
**Schneider, G.** (1998). Cryo X-ray microscopy with high spatial resolution in amplitude and phase contrast. *Ultramicroscopy* **75**, 85-104.
**Slifer, E. H.** (1950). Vulnerable areas on the surface of the tarsus and pretarsus of the grasshopper (Acrididae, Orthoptera) with special reference to the arolium. *Ann. Entomol. Soc. Am.* **43**, 173-188.
**Spurr, A. R.** (1969). A low-viscosity epoxy resin embedding medium for electron microscopy. *J. Ultrastr. Res.* **26**, 31-43.
**Stork, N. E.** (1980). A scanning electron microscope study of tarsal adhesive setae in the Coleoptera. *Zool. J. Linn. Soc.* **68**, 173-306.
**Stork, N. E.** (1983). The adherence of beetle tarsal setae to glass. *J. Nat. Hist.* **17**, 583-597.
**Tian, Y., Pesika, N., Zeng, H., Rosenberg, K., Zhao, B., McGuiggan, P., Autumn, K. and Israelachvili, J.** (2006). Adhesion and friction in gecko toe attachment and detachment. *Proc. Natl. Acad. Sci. USA* **103**, 19320-19325.
**Walker, G., Yule, A. B. and Ratcliffe, J.** (1985). The adhesive organ of the blowfly, *Calliphora vomitoria*: a functional approach (Diptera: Calliphoridae). *J. Zool. Lond.* **205**, 297-307.
**Weiss, D., Schneider, G., Niemann, B., Guttmann, P., Rudolph, D. and Schmahl, G.** (2000). Computed tomography of cryogenic biological specimens based on x-ray microscopic images. *Ultramicroscopy* **84**, 185-197.
**Wilhein, T., Rothweiler, D., Tusche, A., Scholze, F. and Meyer-Ilse, W.** (1994). *Thinned, Back Illuminated CCDs for X-ray microscopy.* In *X-Ray Microscopy IV* (ed. V. V. Aristov and A. I. Erko), pp. 470-474. Chernogolovka, Moscow region, Russia: Bogorodskii Pechatnik Publishing Company.
**Wolter, H.** (1952). Spiegelsysteme streifenden Einfalls als abbildende Optiken für Röntgenstrahlen. *Ann. Phys.* **10**, 94-114.